aerospace

MDPI

Article

Investigation of Merge Assist Policies to Improve Safety of Drone Traffic in a Constrained Urban Airspace

Malik Doole *, Joost Ellerbroek and Jacco M. Hoekstra

Control and Simulation, Faculty of Aerospace Engineering, Delft University of Technology, Kluyverweg 1, 2629 HS Delft, The Netherlands; j.ellerbroek@tudelft.nl (J.E.); j.m.hoekstra@tudelft.nl (J.M.H.)
* Correspondence: m.m.doole@tudelft.nl

Abstract: Package delivery via autonomous drones is often presumed to hold commercial and societal value when applied to urban environments. However, to realise the benefits, the challenge of safely managing high traffic densities of drones in heavily constrained urban spaces needs to be addressed. This paper applies the principles of traffic segmentation and alignment to a constrained airspace in efforts to mitigate the probability of conflict. The study proposes an en-route airspace concept in which drone flights are directly guided along a one-way street network. This one-way airspace concept uses heading-altitude rules to vertically segment cruising traffic as well as transitioning flights with respect to their travel direction. However, transition flights trigger a substantial number of merging conflicts, thus negating a large part of the benefits gained from airspace structuring. In this paper, we aim to reduce the occurrence of merging conflicts and intrusions by using a delay-based and speed-based merge-assist strategy, both well-established methods from road traffic research. We apply these merge assistance strategies to the one-way airspace design and perform simulations for three traffic densities for the experiment area of Manhattan, New York. The results indicate, at most, a 9–16% decrease in total number of intrusions with the use of merge assistance. By investigating mesoscopic features of the urban street network, the data suggest that the relatively low efficacy of the merge strategies is mainly caused by insufficient space for safe manoeuvrability and the inability for the strategies to fully respond and thus resolve conflicts on short-distance streets.

Keywords: urban airspace design; constrained airspace; advanced air mobility; delivery drones; flying taxis

Citation: Doole, M.; Ellerbroek, J.; Hoekstra, J.M. Investigation of Merge Assist Policies to Improve Safety of Drone Traffic in a Constrained Urban Airspace. *Aerospace* **2022**, *9*, 120. https://doi.org/10.3390/aerospace9030120

Academic Editor: Michael Schultz

Received: 21 December 2021
Accepted: 22 February 2022
Published: 25 February 2022

1. Introduction

Advanced air mobility concepts, such as autonomous drones could play an essential role in future express package delivery missions, for example, medical and meal delivery in urban areas [1–5]. The large-scale adoption of drones for urban delivery missions could potentially help reduce traffic congestion and thus decrease total anthropogenic CO_2 emissions in cities [6,7]. In contrast to traditional and contemporary transport modes, such as vans and bikes, drones appear to be flexible and cost effective; moreover, they are easily scalable and comparatively less challenging to automate than road vehicles [8]. Yet, the radical changes promised by autonomous delivery drones may only begin to have profound and extended effects on society and its urban environment when deployed in large-scale. Before widespread adoption of delivery drones unfolds in cities, however, there are many challenges to overcome. As urban environments are densely populated with dynamic and static obstacles [9], operating high densities of drone-based deliveries in a confined space presents a safety hazard to urban occupants [10]. Therefore, this raises the question of how to safely accommodate high-density drone traffic in a constrained urban environment. One logical step forward is to have a suitable urban airspace structure as a means to support these flying robots in dense cities [8].

Previous studies have addressed some of these concerns by proposing corridors and sky-lanes [11,12] and even advocating conceptual rules-of-the-road, such as giving priority for traffic on the right at intersections as a potential means to safely navigate through urban areas [13]. Some have suggested single altitude lane-based approaches that primarily investigated trajectory scheduling algorithms in a way to tackle strategic conflict management [14,15]. While others have focused on conceptual design studies into the use of airway routes over buildings, railways and roads for the city of Singapore [16,17], a majority of the work has been centred on policy-based studies for Europe's advanced air mobility traffic management program, U-Space [18–21]. However, the common thread in these studies is that they are mainly limited to very low traffic densities of drones or even single drone flight operations.

In contrast, quite a large number of studies have been conducted for autonomous flying vehicles operating in unconstrained airspace. The Metropolis project demonstrated that vertical segmentation of cruising traffic according to heading directions leads to favourable levels of safety [22,23]. In a follow-up study, it was revealed that two principles were primarily associated with lowering the conflict probability, namely, the segmentation of traffic into separate parts of airspace (e.g., geofenced areas and layers of airspace) and the reduction of relative velocities by alignment of traffic within the same airspace segment [24,25].

The current paper is part of a project that aims to apply the findings of the Metropolis project to constrained airspace, where vehicles are restricted to flying along the streets. Many of the challenges faced with large-scale drone operations in highly constrained environments are also present in road transportation [26,27], especially in automated road vehicles [28,29]. Because of this, a previous study, which is also part of the current project, combined the Metropolis research of unconstrained urban airspace with principles of road traffic engineering, to propose an implementation of a two-way and one-way airspace configuration [30]. The one-way concept featured horizontal constraints to promote unidirectional traffic within a street, while the two-way concept did not include horizontal constraints and thus allowed for bidirectional flows of traffic. Both concepts feature transition altitudes to accommodate turning traffic that requires a deceleration to perform turns at intersections. By separating slower turning traffic from the main flow, these transition altitudes aim to mitigate any interruptions to the flow of through-traffic. However, in a follow-up study, it was shown that, despite the presence of transition altitudes, the layered airspace structure generated a large number of merging type conflicts when flights transition between layers for a turn [31]. The current paper aims to manage and mitigate the occurrence of merging conflicts through the use of merge assist strategies.

By extrapolating work conducted in highway merging traffic research [26,32–35], we investigated the use of a delay-based and speed-based merge assist framework for a large-scale drone traffic simulation study. Using fast-time simulations, we tested these merge assist policies for low, medium and high traffic densities with respect to the total number of conflicts, intrusions and their constitute properties. Our study not only investigates the macroscopic properties of the network but also examines specific hotspot regions of the network, which features many individual drones interacting in a confined space by following a set of rules, and thus, we uncover key mesoscopic properties of the urban network.

In this work, we perform our research in the context of emerging drone delivery missions, which have the potential to generate high-density traffic scenarios in constrained urban spaces [36]. We use this scenario to evaluate the airspace design and the proposed merging-assist frameworks with low, medium and high traffic densities. Note that this potential scenario of drone delivery is just an example, used in this study to generate sufficiently dense and complex traffic patterns. Other advanced air mobility concepts, such as flying taxis [37] may also exhibit high traffic densities in a constrained urban airspace [38]. The aim of these scenarios is to understand how individual drones interact with each other in a given confined environment and how specific operating rules might trigger undesired emergent behaviour with high traffic densities.

The remainder of this paper is structured, as follows: Section 2 outlines the background material of this study. In Section 3, we present the methodology of our study. In particular, Section 3.2 describes the merge assistance framework and Section 4 gives details about the simulation environment and its set-up. Section 5 presents the results of our experiments. The main findings of our study are then discussed in Section 6. Section 7 summarises the main conclusions of this study.

2. Background

In this section, we summarise relevant background material. We start with a brief description of important airspace safety metrics. Then, we discuss how traffic segmentation and alignment help achieve intrinsic safety by preventing the onset of conflicts. Thereafter, we discuss the one-way airspace concept for high-density drone traffic operations and its associated emergent behaviour when applied to a constrained urban environment.

2.1. Conflicts and Intrusions

The number of pairwise conflicts and intrusions are metrics to describe the safety of an airspace. Here, an intrusion, or a loss of separation, occurs when the horizontal and vertical separation margins are simultaneously violated. A conflict is defined when the horizontal and vertical separation distances between drones is predicted to be violated within a prescribed 'look-ahead' time. Therefore, a conflict can be viewed as an anticipated intrusion.

2.2. Application of Traffic Segmentation and Alignment

Previous studies have extensively investigated the effect of traffic segmentation and alignment as a potential means to increasing the intrinsic safety of the airspace [24,25,39]. Here, we describe traffic segmentation and alignment using the mathematical expression represented by Equation (1).

$$CR_{global} = \frac{1}{2}N(N-1)p_2 \tag{1}$$

In Equation (1), the global conflict rate (CR), or probability of conflict, is related to two parameters. The parameter N indicates the number of vehicles, or drones, in the observed area. Parameter p_2 denotes the probability that any two vehicles in the observed area meet each other, which is dependent on the structure of the routes and airspace. By examining Equation (1), it can be seen that, for a given volume of airspace, increasing N causes a quadratic increase in CR while increasing p_2 causes a linear increase in CR.

The conflict probability can therefore be mitigated by effectively reducing N and p_2 [24,25,39]. A reduction in N can be achieved by the segmentation of traffic, which effectively decreases the likelihood of any possible number of combinations of vehicles that can meet each other within the given airspace. The parameter p_2 has been shown to be composed of factors such as the separation margin and look-ahead time and of the degree of alignment of trajectories, which can be achieved by reducing the relative speeds between two vehicles in the observed airspace [24].

2.3. Challenges of Constrained Urban Environments

In previous research, the principles of segmentation and alignment were applied to an unconstrained or free airspace [22,23]. In contrast, drone-based delivery traffic is expected to utilise a highly constrained urban environment that harbours a large presence of dynamic and static obstacles as well as temporary and permanent no-fly-zones [9]. To an extent, it shares these operational conditions with autonomous cars [29] and traditional road vehicles [26,27,40,41].

Because of the similarities with road traffic, a previous paper in this study explored the consequences of using existing urban street networks and thus 'flying-over-streets' in constrained urban spaces [30]. However, allowing high densities of drone traffic to simply operate in a constrained airspace without any imposed structure would severely impact

the level of safety. To prevent the onset of conflicts, the aim of the previous study was to apply the principles of segmentation and traffic alignment to the urban airspace to organise traffic into different altitude layers with respect to travel directions.

2.4. One-Way Airspace Design

Based on the findings of unconstrained urban airspace research [22,23] and road traffic studies [32,42,43], we developed a one-way airspace configuration. Historically, one-way streets have been adopted as a simple and efficient measure to manage traffic safety in urban networks [44]. Here, drone flights are directly guided over one-way streets while adhering to the urban street network. To separate traffic according the four quadrants of north, east, south and west directions, the airspace is vertically segmented into a stack of direction-constrained altitude layers. In addition, a one-way directional constraint is imposed on each street, where a street only accommodates north, east, south or westbound traffic. This means that opposite traffic flows are not separated by means of altitude but instead guided along (parallel) streets [30], which is comparable to one-way street traffic for on-ground traffic [42]. In this research, we use an orthogonal grid-like network, such as the Manhattan urban street network, because it is predominately optimised for one-way traffic [45].

2.4.1. Through and Turn Altitude Layers

In this study, the airspace is divided into two main types of altitude layers consisting of through-layers, which accommodate through traffic; and turn-layers, which is necessary to facilitate turning traffic (see, Figure 1). Here, we define through traffic as traffic that travels across at least one intersection, while turning traffic is denoted by traffic that is turning at an intersection. In our experiments, turning traffic is required to decelerate and thus reduce speed to safely execute a turn at an intersection. Separating slow turning traffic from through traffic reduces the conflict probability and thus also decreases any potential disruptions between the two flows, which in turn increases the safety of the airspace. Notably, a similar design approach is seen in highway design for road vehicles [26].

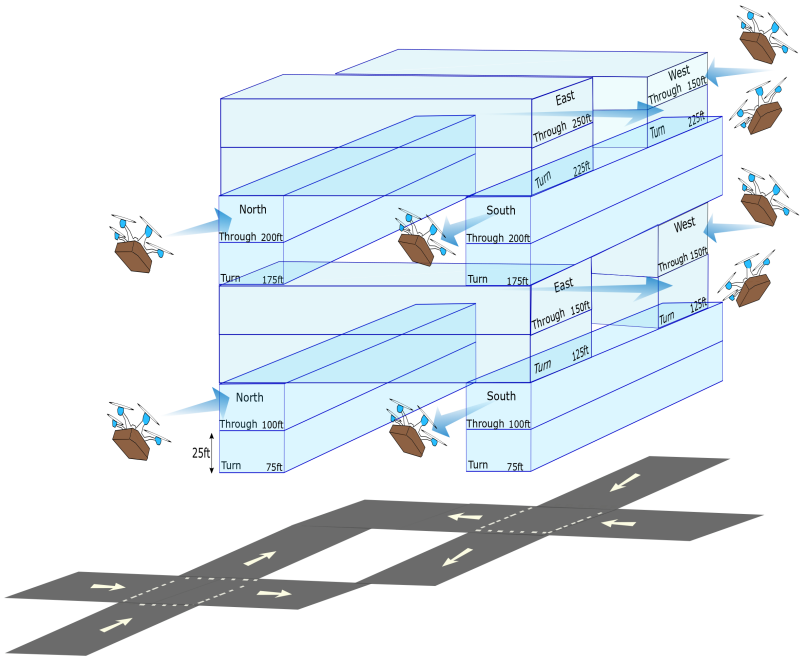

Figure 1. Schematic 3D view of one set (75 to 250 ft) of altitude layers for the one-way urban airspace design configuration, where each altitude layer corresponds to the respective travel direction. Note that the airspace configurations consist of through-layers and turn-layers. Through-layers are used by through traffic which passes through at least one intersection. While the turn-layers are utilised by transitory flights, that is, flights that need to perform turns at the respective intersections.

2.4.2. Altitude Layer Assignment

In this study, the flight routes coincide with the urban street network, i.e., the drone flights are directly guided along the streets. Hence, it is assumed that the layers are not hindered by any buildings and it only conforms to the street network.

The airspace concept in this study consist of multiple stacks of altitude layers that range from 75 to 1050 ft. Moreover, the airspace features through-layers and turn-layers that are vertically spaced at a distance of 25 ft. As a result, this implies that the airspace concept can hold 40 layers, which comprises 20 through-layers and 20 turn-layers, respectively. Within these 40 layers, there exist 20 layers for each cardinal direction. Therefore, the number of layers depend on the assumed altitude range (i.e., 75 to 1050 ft) and the vertical separation distance of 25 ft. In Figure 1, we present a schematic 3D illustration of one set altitude layers that fit into the altitude range 75 to 250 ft for the one-way airspace concept. To obtain the complete set of 40 altitude layers, the set of eight altitude layers is repeated five times until 1050 ft [30].

Note that, although different choices can be made in selecting these values, this only affects the number of layers available to each cardinal direction. It does not change the main principle of the airspace concept. The reasons for selecting this particular altitude range are that the definition of clear altitude airspace for drones to operate varies with respect to region [46]. Additionally, the U-Space concept of operations study has not defined the boundaries of the airspace for which drones are assumed to operate [19].

The allocation of altitudes is based on the respective flight headings; hence, we employ a simple altitude-heading rule to compute the flight altitudes ($h_{OW,i}$):

$$h_{OW,i} = h_{min} + \frac{h_{max} - h_{min}}{d_{max} - d_{min}}(d_i - d_{min}) \tag{2}$$

where h_{max} and h_{min} are the maximum and minimum altitude of the through-layers, d_i is the shortest path distance between the respective origin–destinations, while d_{min} and d_{max} are the minimum and maximum threshold distances to the respective origin–destinations. This equation ensures that shorter flights are allocated to lower altitudes and longer flights are allocated to higher altitudes. Next, we use a basic heuristic, as illustrated by Algorithm 1, to assign the flight altitudes according to their respective heading direction. Note that ζ denotes the vertical distance (25 ft) between layers.

Algorithm 1: Heuristic to align flight altitudes to their travel direction.

if $315^\circ < \psi \leq 045^\circ$ or $135^\circ < \psi \leq 225^\circ$ **then**
  $h_{OW,i} = h_{OW,i}$
else
  if $045^\circ < \psi \leq 135^\circ$ or $225^\circ < \psi \leq 315^\circ$ **then**
    $h_{OW,i} = h_{OW,i} + \zeta$
  end if
end if

2.5. Emergence in the One-Way Airspace Design in Constrained Environments

The one-way airspace design is made up of different rules and interventions to safely facilitate large-scale drone traffic in a constrained urban environment. In particular, the altitude-heading rule and the spatial order of the urban street network is used to enforce traffic segmentation and alignment. Consequently, this requires drones to climb and descend to their respective altitudes, which in turn introduces merging conflicts. In addition, the airspace is composed of transition altitude layers to safely harbour turning flights. However, this design feature could lead to the onset of additional merging conflicts as flights need to frequently ascend and descend from through to turn-layers and turn to through-layers before and after every heading change. Furthermore, a speed-based algorithm is used for tactical resolution which can trigger 'knock-on' conflicts. Therefore, it must be acknowledged that these seemingly simple geometrical rules on a drone and its interaction with the airspace system can also trigger undesired emergent behaviour [47,48].

3. Merging Conflicts and Intrusions

In a previous study, we demonstrated that a large proportion of conflicts in the one-way airspace design is caused by merging flights, that is, drones that are climbing and descending to their respective altitude layers [31]. In this section, we present our methodology to identify and circumvent the potential merging conflicts and intrusions. For this, we use a time-space diagram to visualise potential merging conflict and intrusion events [26,32–35,49,50]. In this section, we describe two merge assist policies aimed at preventing potential merging conflicts.

3.1. Time–Space Diagram

A time–space diagram is a graph that describes the position of a vehicle and its progression in time along a particular traffic stream. Time–space diagrams are typically used in road traffic engineering as a visual tool to analyse and select optimal coordination strategies for traffic signals [26]. The tool is also used in other transportation domains, such as airports to measure runway capacity [51]. Time–space diagrams are also explored in Air Traffic Management (ATM) research as a controller support tool for continuous descent operations to determine the ideal separation distances for merging traffic [52]. In this study, a time–space diagram is employed to visualise the trajectories of a pair of drones and thus to help circumvent a potential merging conflict, see Figure 2.

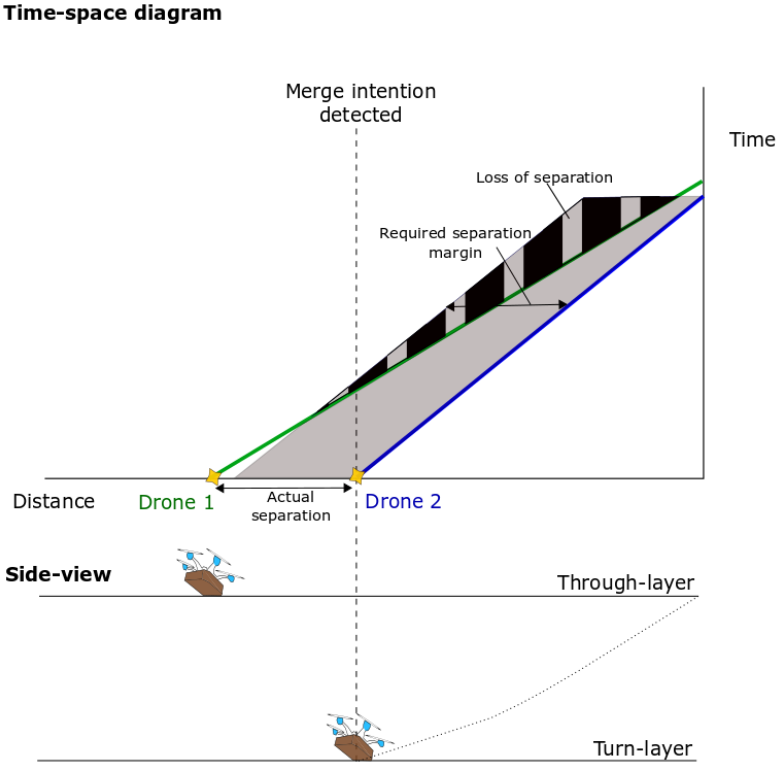

Figure 2. Example of a time–space representation for a pair of drones. The flight trajectories of drone 1 and drone 2 are represented by the green and blue lines. The grey area denotes the required separation margin, while the shaded area depicts a separation violation. To maintain safe separation, the trajectories need to be within or outside the required separation margin (grey area). Note that a side-view is only included for purpose of clarity.

Figure 2 illustrates a typical scenario observed in the one-way airspace design. It shows a drone transitioning from its respective turn-layer to a through-layer. The diagram shows the trajectories of drone 1 (green line) and drone 2 (blue line) and their required separation margin (grey area). As drone 2 initiates a climb, the separation margin decreases, hence triggering a loss of separation, as illustrated by the shaded region in Figure 2. The time–space diagram reveals a few approaches to mitigate the merging conflict and intrusion by influencing the

trajectories of the respective drone flights. Essentially, we can influence the speeds of the drones and hence tilt and slant the lines, which effectively ensures that the drones stay within or outside the required separation margin, to circumvent a conflict. Alternatively, we can shift the lines along the time axis by imposing a delay in effort to maintain the required separation margin. Therefore, in this study, we aim to influence the speed of the merging drone and to delay the merging process in order to prevent merging conflicts.

3.2. Merge Assistance Policies

A safe merge event is attained by having sufficient spacing in the intended traffic flow to accommodate the merging vehicle. Here, we propose two types of merge assist policies, which is inspired by road traffic research [26,32–35], to generate sufficient spacing to form a 'gap' in the traffic stream in order to safely merge. In the first merge assist policy, we implement a speed-based strategy to generate the desired gap for traffic to safely merge (see sketch of proposed Algorithm 2) by decelerating the merging drone until the desired gap is attained and thus allowing it to safely merge into the respective traffic layer.

Algorithm 2: Speed-based merge assistance policy.

Data: n = number of drones; ID_k = drone identification number for all traffic $\forall_k = \{0, \ldots, n\}$; ID_m = drone identification number for merging drones $\forall_m = \{0, \ldots, n\}$; ID_{nm} = drone identification number for non-merging drones $\forall_{nm} = \{0, \ldots, n\}$; m = merging drone; nm = non-merging drone; $altCur$ = current altitude; $altTar$ = target altitude; Δh = altitude difference; v_m = speed of merging drone; v_{nm} = speed of non-merging drone; τ = minimum gap that is estimated to be the cruise speed multiplied by the look-ahead time;

For each simulation time-step:
Retrieve all drone ID_k and get $taralt$ of next way-point;
if $|altCur - altTar|$ *for each drone* > 0 **then**
  Potential merge expected ;
  Get drone ID_m of merging drone;
  $ID_m \longleftarrow$ store identification number;
  for *each merging drone (m)* ID_m **do**
    Check traffic in $altTar$ of ID_m;
    Compute traffic in $altTar$ of ID_m;
    $altTar \longleftarrow$ store target altitude layer traffic;
    Get non-merging ID ID_{nm} in $altTar$;
    $ID_m n \longleftarrow$ store identification number;
    if *gap between merging m and non-merging nm* $< \tau$ *and* Δh $\leq \zeta$ **then**
      Potential merging conflict predicted;
      Call speed-based merge-assisting policy;
      Retrieve potential merging IDs (ID_m);
      Decelerate and choose v_m speed from $\in$ [5 m/s, 10.3 m/s] s.t. min gap is generated;
      Check for gap generated between drone m and nm **until**;
      if *gap is sufficient to safely merge* **then**
        Return v_m to original speed assigned in flight plan ;
      end
    end
  end
end

In the second merge assist policy, we employ a delay-based strategy, as summarised in Algorithm 3. This two-pronged approach influences the speed of the merging vehicle, and it instructs the merging vehicle to slow-down and wait in its respective altitude layer

until it is safe to merge. Then, once a gap is formed, the merging drone safely transitions to its respective altitude layer. Depending on the velocity difference between the merging and non-merging drone (i.e., the vehicle in the through traffic layer), this merging drone then positions itself either behind or in-front of the non-merging vehicle. A similar approach is applied for ramp traffic that waits until a desired gap is found to enter the highway [53]. However, despite this similarity, road traffic and its individual drivers are able to attain the desired gaps to safely merge by using social cues and coordination, such as switching on signal indicators, making relevant eye contact and hand gestures, which are largely missing and challenging to model in autonomous systems [29,54].

Algorithm 3: Delay-based merge assistance policy.

Data: n = number of drones; ID_k = drone identification number for all traffic $\forall_k$ = {0, . . ., n}; ID_m = drone identification number for merging drones $\forall_m$ = {0, . . ., n}; ID_{nm} = drone identification number for non-merging drones $\forall_{nm}$ = {0, . . ., n}; m = merging drone; nm = non-merging drone; $altCur$ = current altitude; $altTar$ = target altitude; Δh = altitude difference; v_m = speed of merging drone; v_{nm} = speed of non-merging drone; τ = minimum gap that is estimated to be the cruise speed multiplied by the look-ahead time;

```
For each simulation time-step:
Retrieve all drone ID_k and get taralt of next way-point;
if |altCur − altTar| for each drone > 0 then
    Potential merge expected ;
    Get drone ID_m of merging drone;
    ID_m ⟵ store identification number;
    for each merging drone (m) ID_m do
        Check traffic in altTar of ID_m;
        Compute traffic in altTar of ID_m;
        altTar ⟵ store target altitude layer traffic;
        Get non-merging ID ID_nm in altTar;
        ID_mn ⟵ store identification number;
        if gap between merging m and non-merging nm < τ and Δh ≤ ζ then
            Potential merging conflict predicted;
            Call delay-based merge-assisting policy;
            Retrieve potential merging IDs (ID_m);
            if Check altCur is current turn-layer then
                Stay in current turn-layer;
                Decelerate and choose v_m speed from ∈ [5 m/s, 10.3 m/s] s.t. min
                 gap is generated;
                Check for gap generated between drone m and nm until
                if gap is sufficient to safely merge then
                    Return to original flight plan ;
                end
            end
            if altCur is current through-layer then
                Decelerate and choose v_m speed from ∈ [5 m/s, 10.3 m/s] s.t. min
                 gap is generated;
                Check for gap generated between drone m and nm until
                if gap is sufficient to safely merge then
                    Return to original flight plan ;
                end
            end
        end
    end
end
```

4. Simulation Design

The performance of the merge assistance strategies is compared in a set of fast-time simulations, with respect to safety for low, medium and high traffic demand. In this study, we approach our experiments by first investigating the extent to which tactical conflict resolution is able to circumvent merging conflicts and intrusions. Thereafter, we augment the tactical conflict resolution with the merge assisting policies in an effort to largely reduce the merging conflicts and intrusions. In this section, we describe the design and development of our experiments used in this study.

4.1. Simulation Development

4.1.1. Simulation Platform

To conduct fast-time simulations, we used BlueSky [55,56], which is an open-source ATM simulator that has been widely employed in past ATM-related studies [22,23,39]. The BlueSky traffic simulation tool is therefore used as the simulation platform. For the purpose of this study, we updated BlueSky's autopilot module to include elements that are specific to unmanned traffic management such as, for example, a suitable drone model and relevant drone dynamics, to account for safe manoeuvrability of flights.

A majority of drone delivery studies and prototypes presented by drone companies mainly assume them to be multi-copters [57–59]. The primary reason for this could be attributed to the rotorcrafts' flexibility, that is the ability to hover and easily manoeuvre the complex urban landscape compared to fixed-wing drones. Therefore, to be in-line with past research, we employ a multi-copter drone model in this study. In particular, we use the DJI Matrice 600 Pro hexacopter, which can be easily modified to transport packages. The characteristics of this drone model are presented in Table 1.

Table 1. Performance data for DJI Matrice 600 Pro used in the simulations of this study.

Parameter	DJI Matrice 600 Pro
Speed [m/s]	5–10.3
Vertical speed [m/s]	−5–5
Mass [kg]	15
Maximum bank angle [°]	35
Acceleration/deceleration [m/s^2]	3.5

4.1.2. Testing Region

In this study, we investigate the performance of the merge assistance strategies for the one-way urban airspace concept. To simulate a constrained urban environment, we apply the urban airspace concept to the urban street network of Manhattan, New York city (see Figure 3). There are three main advantages for selecting Manhattan as our testing region. First, Manhattan has an orthogonal network structure, and thus, it contains fewer dead-ends, more four-way intersections and less-winding street patterns [45]. In comparison with other cities, such as Paris or Rome, the highly ordered grid-like street orientations of Manhattan reduce ambiguities in our findings [60,61]. Second, Manhattan is widely utilised by advanced air mobility studies as a testing region in their simulations [62–64]. Third, the construction of new streets are increasingly orthogonal in nature [65–67]. Therefore, the findings of this study would still be valid in future cities.

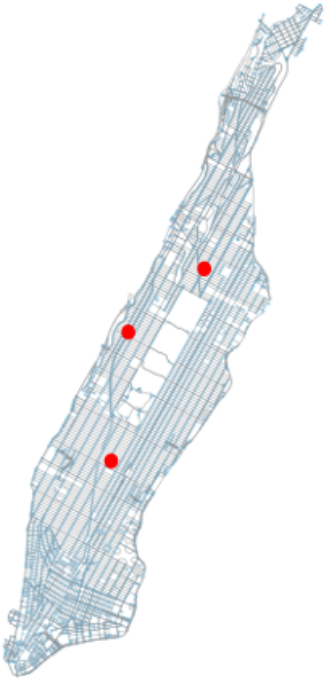

Figure 3. Urban street network of Manhattan, New York City (with area size of 59.1 km^2), generated from OpenStreetMap data [68] via OSMnx Python library [69]. The three red dots represent the (approximate) location of chosen drone depots in our study.

4.1.3. Conflict Detection and Resolution

In our study, a 'state-based' conflict detection method is employed to identify potential separation violations [48,70] by linearly extrapolating the drones' state within a prescribed 'look-ahead' time. Using a linear extrapolation method means that there is a likelihood that false conflicts could be detected, and therefore, it would need to be identified in the post-processing phase of this study. In addition, we employ separation requirements of 82 ft and 24 ft for the respective horizontal and vertical separation boundaries. The above separation requirements were adopted based on trial experiments since no formal separation distance standards have been established for autonomous delivery drone flights in constrained outdoor environments. A prior study employed horizontal separation values of 105 ft and 164 ft [71,72], while other studies have used values ranging between 16 and 984 ft for the vertical separation requirement [14,73]. Note that the separation distance can affect the proper functioning of conflict detection and resolution in constrained airspace, through its relationship with aspects such as the traffic density; the performance characteristics of the drones; and the topology of the network, for example, the length of the streets. For the experiment area of Manhattan, the majority of the street lengths range between 17 and 140 ft. With larger horizontal separation distances, the linear state-based conflict detection method would detect false conflicts, which do not even result in a loss of separation because of the topology of the airspace structure. Therefore, in this study, the horizontal separation distance of 82 ft and vertical separation distance of 24 ft proved optimal in terms of the number of losses of separation prevented and the false conflicts detected. The detected conflicts are then resolved in a pair-wise manner using a basic (1-D) speed control algorithm, as described in Algorithm 4.

4.1.4. One-Way Airspace Concept Implementation

The network geometries of Manhattan were extracted from OpenStreetMap (OSM) [68] using the OSMnx Python package [69], which provides an interface to query OSM data. We then used the OSMnx package to extract nodes and edges to generate a graph for Manhattan. The network graph of the one-way concept featured a directed graph, and thus, it enforces the streets to be one-way.

Algorithm 4: Basic (1-D) speed control conflict resolution.

Data: n = number of drones; v_j = speed of drone j; $nconf$ = number of conflicts; $confpair$ = conflict pair of i, j where i is the leader drone and j is the follower drone;
Require n, v_j $\forall_j = \{1, \ldots, n\}$
Compute and get $nconf$ and conflict pairs from state-based conflict detection
if $nconf > 0$ **then**
  for *all conflict pairs get drone j of conflict pair* ($\rightarrow$ *compute new* v_j) **do**
    if $confpair\ i, j$ *in current conflict* **then**
      change v_j to have speeds from $\in$ [5 m/s, 10.3 m/s] s.t. min separation is respected between drone i and j ;
      if $confpair\ i, j$ *not in current conflict* **then**
        Return j to original speed assigned in flight plan ;
      end
    end
  end
end

Three depot locations that were based on initial experiments that demonstrated convergence of traffic flow were chosen for this study. During the simulation, all drone flights departed from one of the three depots to their respective destinations, which includes a set of uniformly distributed destinations that adhere to the drones' minimum and maximum range limit of 1 km and 10 km. Note that this study does not consider take-off and landings phases and that it only considers en-route flights phases.

Therefore, in this study, each drone in the simulation was created at its respective cruising altitude at each of the three depots. Then, the respective drone followed its respective flight plan and flight route. Based on the respective depot location and the destination, we computed the shortest paths using the method described in [74]. Each shortest path consisted of a set of geographical coordinates, which were used to determine the bearing (heading direction) of each of the streets along the shortest path; and the distance of the shortest paths. Once the drone arrived at its respective destination location, it was deleted from the experimental area.

4.2. Independent Variables

Three independent variables were considered in this study:

1. Airborne separation assurance conditions: with and without tactical conflict resolution;
2. Merge assistance strategies: speed-based and delay-based assistance; and,
3. Traffic demand: low, medium, and high traffic densities.

In this work, we based the traffic demand on food-delivery scenarios [8,36]. Such applications have been widely investigated by startups and large technology companies. Table 2 summarises the traffic demand scenarios used in this study for the city of Manhattan, which encompasses an area of 59.1 km^2. Note that, even though in this case, food delivery is chosen as a scenario, this traffic demand could also represent different applications, such as parcel delivery, or a potential medical-delivery scenario, in which drones rapidly deploy vaccines or any other time-sensitive medical material to patients or between hospitals [75].

The combination of the three independent variables results in 12 experimental conditions. Each condition was performed with five different traffic realisations, resulting in a total of 36 simulation runs (two conflict resolution conditions $\times$ two merge assistance strategies $\times$ three traffic demand cases $\times$ three repetitions). The randomisation between traffic realisations was performed by uniformly and randomly generating origin–destination pairs between depots with distances ranging from 1 km and 10 km for the city of Manhattan.

Table 2. Traffic density characteristics of the three demand scenarios for the simulation area of Manhattan, New York City, network consisting of an area of 59.1 km^2.

	Low	**Medium**	**High**
Traffic density (drones/km^2)	31	46	61
Inflow rate (drones/min)	30	45	60
Hourly demand (drones/h)	1800	2700	3600
Demand per depot (drones/depot)	600	900	1200

4.3. Dependent Measures

In this study, we consider several dependent measures related to safety, which consist of the total number of pairwise conflicts and intrusions, to evaluate the performance of the merge assist policies.

4.3.1. Safety

The safety of the airspace is measured in terms of the total number of pairwise conflicts and intrusions. In this study, a better merge assist policy is determined by fewer conflicts and intrusions. Here, an intrusion, or loss of separation, occurs when there is a violation of the minimum vertical and horizontal separation requirements. While, a conflict is a predicted loss of separation within the predefined look-ahead time. For our experiments, we employ a look-ahead time of 10 s. A look-ahead of 10 s implies that the drones need to look ahead at a distance of about 100 m when cruising. This look-ahead time is tuned to the average length of the street for the experiment area of Manhattan. With a larger look-ahead time the state-based conflict detection looks at distances beyond the average street length, thus triggering many false conflicts. As a result, in our study, a look-ahead time of 10 s demonstrated the optimal balance between the number of false conflicts being detected and the number of intrusions prevented in a trial simulation experiment.

4.3.2. Distance between the Nearest Drone Pair on the Same Altitude Layers

Here, we capture the distance to the nearest drone within the same altitude layer per street, for low, medium and high traffic demand. We use this metric to understand the distance distribution of pairs of drones that fly at distances smaller than horizontal separation distance (82 ft) in all directions. We speculate that pairs of drones that fly below this threshold value have limited manoeuvrability for safe merging.

4.3.3. Traffic Accumulation per Street

Together with the distance between the nearest drone pair mesoscopic property, we also measure the accumulation of traffic on a particular street, that is, the number of drones flying over a street within its respective altitude layer. During the initial simulation phase, we observed some streets that experienced disproportionately higher traffic flows. To quantify the traffic flow in such streets, we measured the local traffic flow in one particular street in our experiment region.

4.4. Experimental Hypotheses

Our working hypothesis related to this study is that a larger number of conflicts, intrusions and conflict chains would be seen with increasing traffic demand. Furthermore, we hypothesise that applying the delay-based and speed-based merge assist policies, along with tactical conflict resolution, would demonstrate a marked decrease in the total number of conflicts and intrusions for low, medium and high traffic demand cases. In addition, we hypothesise that the speed-based merge assist policy would have better performance than the delay-based policy. Because in the delay-based merge assist policy, a merging flight has to lower its speed and thus to prolong its time spent in the turn-layer until it is safe to merge and thus as traffic density increases, it is likely that a larger proportion of in-trail conflicts would be triggered when merging.

5. Results

The experimental results of this study are presented in this section. The effect of the independent variables on safety is illustrated using stacked bar charts, scatter plots and box-and-whisker plots for the distance between the nearest drone measures. In each box-and-whisker plot, we display the median line; interquartile range (IQR), which is captured by the bounds of the box and represents the 25–75th percentiles; the minimum and maximum distribution of the data, denoted by the whiskers; and the points greater than $\pm 1.5 \times$ IQR, representing outliers. The different categories of conflicts and intrusions are depicted using stacked bar charts, and the spatial distribution of intrusions is illustrated with scatter plots.

5.1. Total Number of Conflicts and Intrusions

Here, we present our results for the total number of pairwise conflicts and intrusions in the one-way airspace design and its effect to the tactical conflict resolution. Figures 4 and 5 therefore depicts these safety metrics for the one-way urban airspace concept for low, medium and high traffic demand cases. In this study, a pairwise conflict and intrusion is accounted for only once during the simulation, while a repeating pairwise conflict and intrusion is recounted, independent of its duration. Figure 4 illustrates an increase in the total number of pairwise conflicts with increasing traffic demand. This same trend is observed in the total number of pairwise intrusions, as shown in Figure 5.

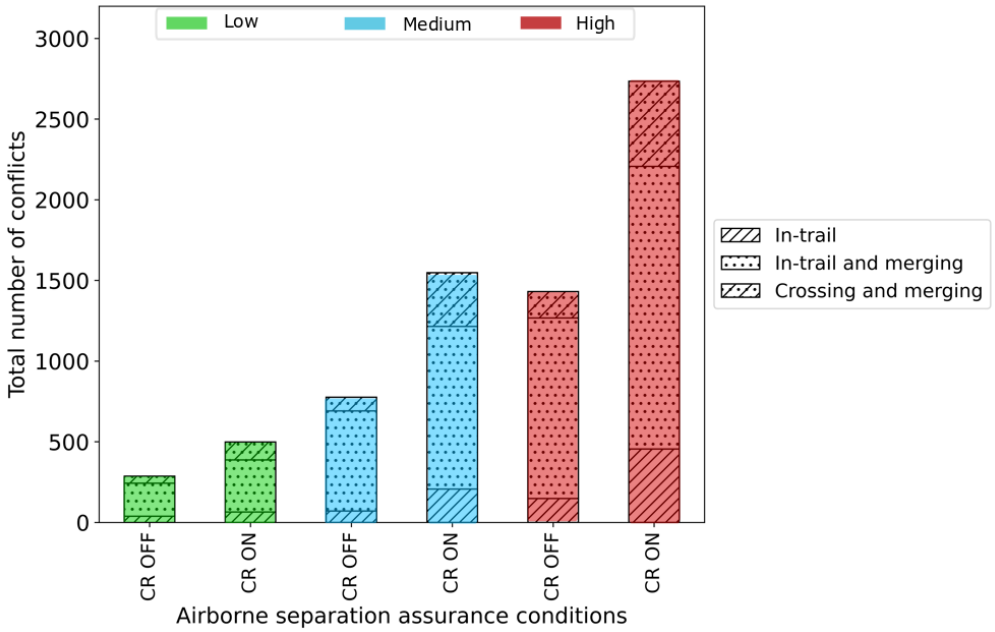

Figure 4. The total number of pairwise conflicts and their associated type with (CR ON) and without (CR OFF) tactical conflict resolution for low, medium and high traffic demand.

Figures 4 and 5 demonstrate the effect of the airborne separation assurance conditions, which are represented with (CR ON) and without (CR OFF) tactical conflict resolution for the one-way concept. In addition, Figures 4 and 5 indicate the composition of the conflicts and intrusions to gain a deeper understanding in the total number of in-trail, crossing and merging conflicts, and intrusions. In Figure 5, we observe that, as expected, the total number of intrusions is significantly reduced with tactical conflict resolution. Conversely, an opposite trend was seen in the total number of conflicts. With tactical conflict resolution, the total number of conflicts increased across all three traffic demand cases. This effect is caused by a lack of manoeuvrability for resolution manoeuvres as a result of the highly constrained airspace design. Therefore, the increased structuring of the airspace increases the probability of encountering other drones when tactical conflict resolution is engaged and it eventually

leads to conflict chains and thus secondary conflicts. Note, however, that such knock-on effects are inherent to decentralised reactive systems. [39,70,76–78]. In fact, even centralised separation strategies can trigger secondary conflicts with increasing traffic density [76]. However, it is not necessarily the case that these secondary conflicts are destabilising and detrimental to safety. Their effect can also be positive by communicating the intent to resolve and thus help to create more of a stabilising effect on the airspace [70]. Secondary conflicts are also observed in road traffic for which they also provide a beneficial effect [79,80].

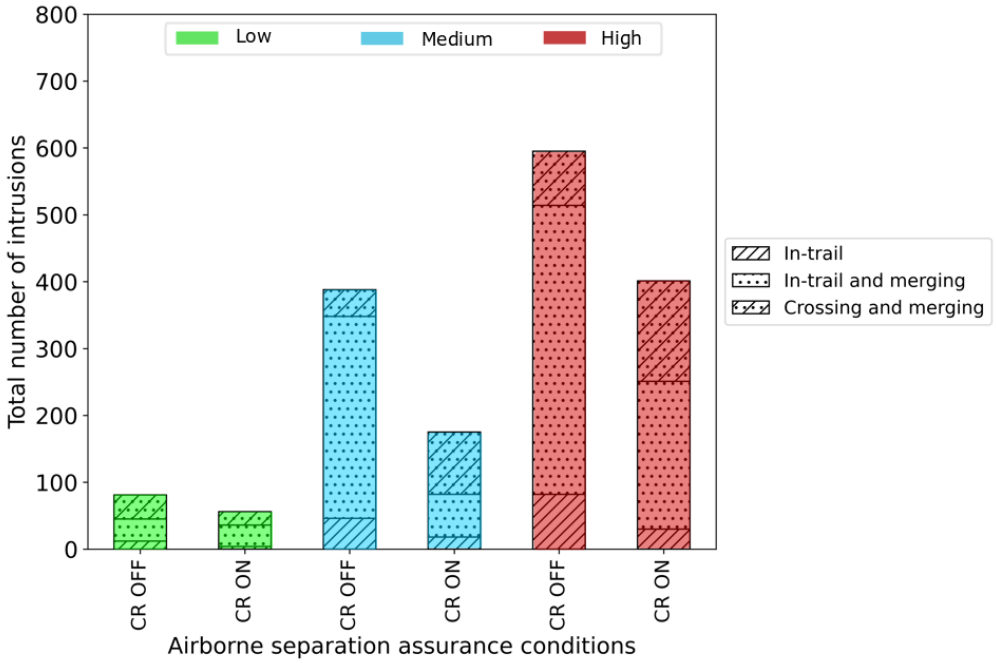

Figure 5. The total number of pairwise intrusions and their associated type with (CR ON) and without (CR OFF) tactical conflict resolution for low, medium and high traffic demand.

5.2. Effect of Merge Assistance Strategies on the Total Number of Conflicts and Intrusions

Next, we present the findings for merge assist policies. Figures 6 and 7 display the effect of the speed-based and delay-based merge assistance polices on the total number of pairwise conflicts and intrusions for low, medium and high traffic demand scenarios. Note that, in all three cases (i.e., MA OFF, MA DELAY and MA SPD), we consider the effect with tactical conflict resolution switch on (i.e., CR ON). In addition, the bar charts categorise and display the proportion of in-trail and crossing types of conflicts and intrusions for level and merging flights. The bar charts show that the conflicts and intrusions are primarily generated by flights that are transitioning to their respective altitude layers because of the large proportion of merging conflicts and intrusions.

Figure 6 shows a modest decrease in the total number of conflicts with delay-based and speed-based merge assistance. In comparison with the scenario of without merge assistance, the total number of conflicts in the delay-based merge policy depicts a 28–38% decrease from low to high traffic demand, while a 29–44% decrease is shown in the speed-based merge policy, for low to high traffic demand. In terms of the categories of conflicts, Figure 6 mainly indicated a decrease in the in-trail and crossing types of conflicts when merging.

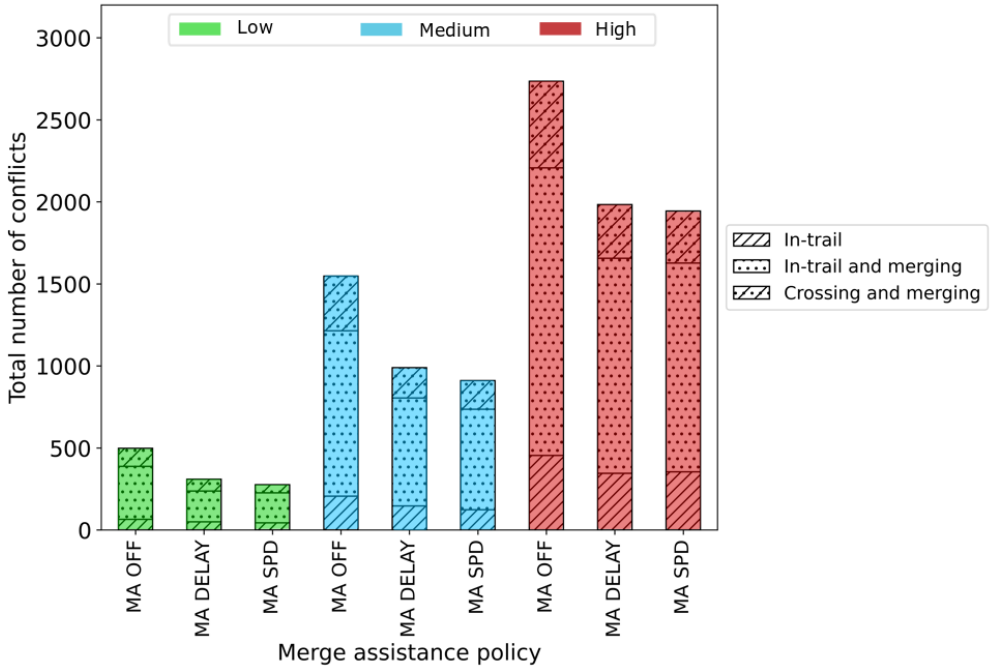

Figure 6. The total number of pairwise conflicts and their associated type with and without merge assistance for low, medium and high traffic demand. Note that MA OFF means without merge assistance. All three cases (MA OFF, MA Delay and MA SPD) also consider the effect of the tactical conflict resolution.

Similarly, the bar chart in Figure 7 demonstrates a less modest decrease for the total number of intrusions in the delay-based and speed-based merge assistance policies. As initially hypothesised, the speed-based policy more effectively reduces the total number of intrusions than the delay-based policy. In comparison to the without merge assistance scenario, the delay-based policy demonstrates a decrease of 6–8% in the total number of intrusions for the low to high traffic demand, while the speed-based policy shows a decrease of 9–16% in the total number of intrusions for low to high traffic demand. In terms of categories of intrusions, we see a slight decrease in the number of intrusions for crossing and in-trail merging flights. However, with higher traffic demand, the number of in-trail type intrusions increases, which could be related to the longer merging process, hence creating bigger speed differences between a pair of drones. Nevertheless, the figures show that the speed-based policy has better performance than the delay-based policy. The better performance can be attributed to the decrease of in-trail conflicts and intrusions when merging since drones do not have to remain in the turn-layers for a safe merge opportunity.

5.3. Spatial Distribution of Intrusions without and with Merge Assistance

We next examined the location of pairwise intrusions without and with merge assistance to determine the potential cause of any unresolved intrusions. To analyse this, we overlaid the exact geographical coordinates of each pairwise intrusion for the high traffic density scenario over our experiment area to locate where these intrusions take place. The charts in Figure 8 represent the geographical location of pairwise intrusions without any merge assistance and with merge assistance for the high traffic density scenario. The plots suggest that most intrusions remain unresolved even with the use of merge assistance at particular locations in the street network. These unresolved intrusions are mainly located in certain hotspot regions, which have a high concentration of intrusions, as seen in the charts. Therefore, the results indicate that the location and geometry of the street network strongly influence the efficacy of the merge assist policies. Hence, to further investigate the latter, we look at the network on a mesoscopic level and thus inspect specific streets that display hotspots.

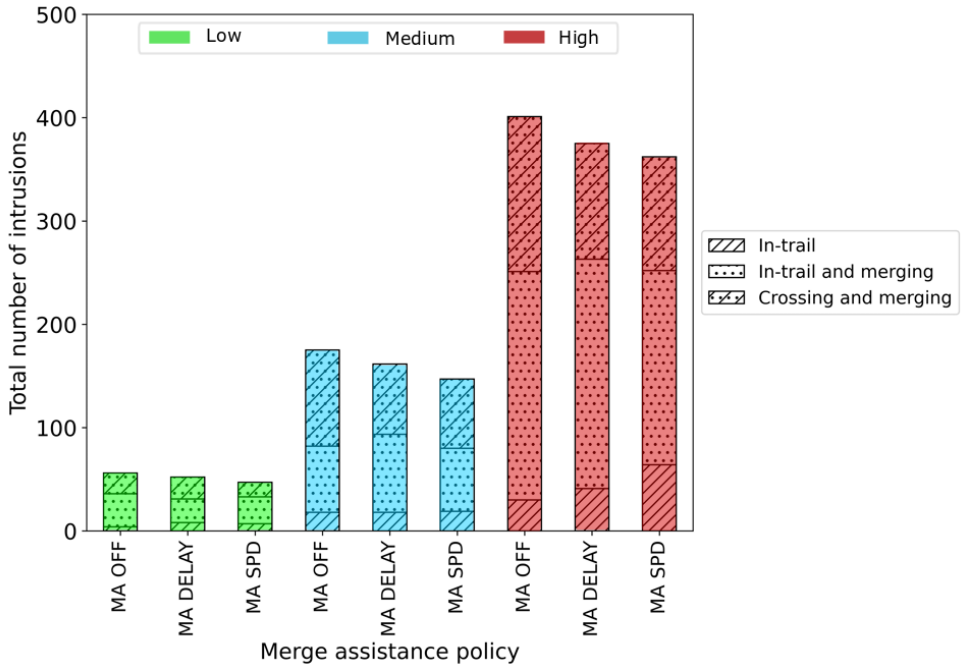

Figure 7. The total number of pairwise intrusions and their associated type with and without merge assistance for low, medium and high traffic demand. Note that MA OFF means without merge assistance. All three cases (MA OFF, MA Delay and MA SPD) also consider the effect of the tactical conflict resolution.

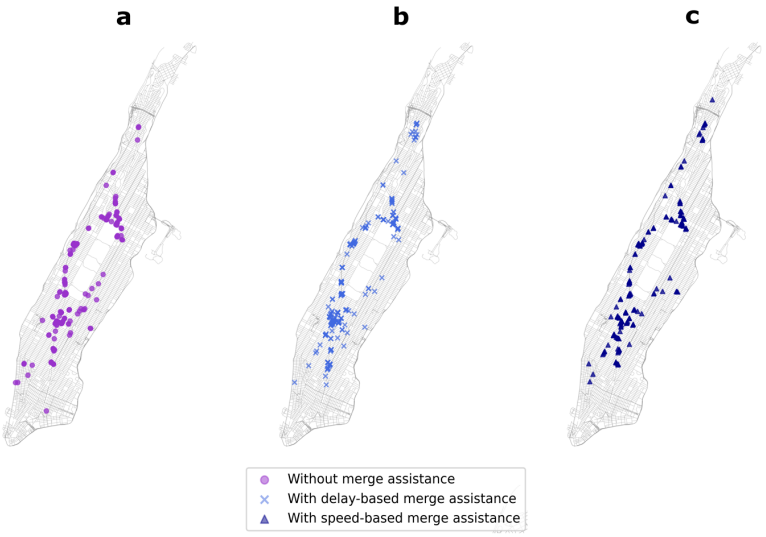

Figure 8. Here, (**a**–**c**) geographical location of pairwise intrusions that relate to without merge assistance, with delay-based merge assistance and with speed-based merge assistance with respect to the high traffic density scenario. Colours are used to distinguish the different pairwise intrusion categories: without merge assistance marked in purple (**a**), delay-based merge intrusions represented by the blue crosses (**b**), and the speed-based merge intrusions marked by the blue triangles (**c**). The overlaid intrusions from the different merge assist policies indicated by the darker hotspot zones demonstrate that some intrusions remain unresolved.

5.4. Mesoscopic Traffic Observations

We next explored why most intrusions remained unresolved in some portions of the urban network. By investigating the mesoscopic nature of the airspace concept, we uncover that a majority of unresolved intrusions mainly exist in busy streets for which the average distance between the nearest drone is less than the horizontal separation distance of 25 m

which is used in our study. These busy streets are identified using a heatmap, as shown in Figure 9. The heatmap illustrates a few hotspot regions. Note that the heatmap is generated using a geographic spatial software [81] by using the Kernel Density Estimation (KDE) to create the heatmap and by setting the search radius (bandwidth) of the KDE to 100 m with a quartic kernel density (i.e., only coordinates within this search radius is used to estimate the KDE and thus generate the heatmap) [82,83]. Here, we examine one specific hotspot area in our experiment, which is depicted in Figure 10. In particular, the charts show a hotspot street where intrusions are largely prevalent even with the use of merge assist policies.

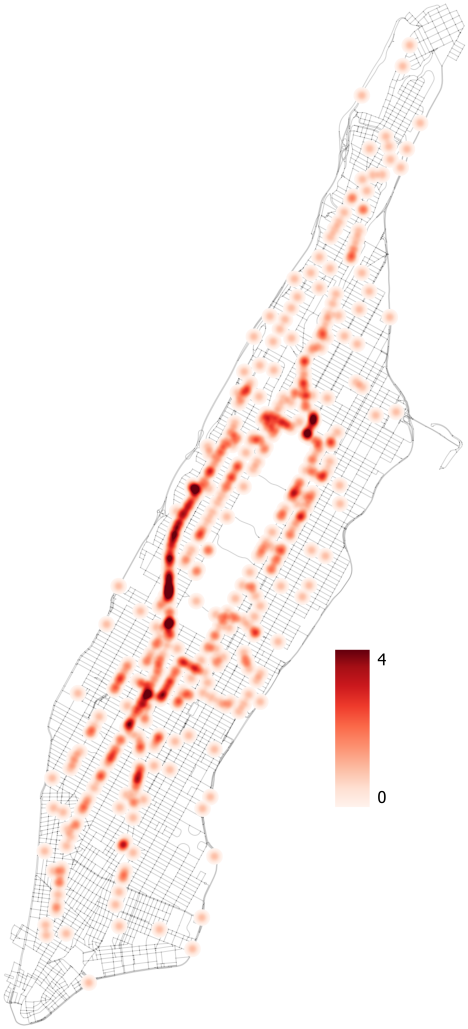

Figure 9. Traffic density heatmap of Manhattan urban network. The colour ramp depicts the traffic density from 1 to 4 drones per street within a search bandwidth of 100 m. The dark red region represents a high volume of traffic, whereas the faded coloured regions indicate low volume of traffic.

In Figure 10, street 'A', which comprises of a length of approximately 63 m, indicates that the nearest drone within the same layer is below the horizontal separation distance of 25 m, as illustrated by the median of the box-and-whisker plot in Figure 10b. Additionally, Figure 10c depicts the traffic density of the street that demonstrate, on average, some layers experience between two to four drones within the street at a particular instance in time. Note that the localised concentration of traffic on particular streets, which cause high traffic densities, is attributed to a specific property of the urban street network [84–87], and thus, the results illustrate that the current routing scheme should also incorporate traffic density in its cost function to prevent traffic hotspots. Therefore, the above findings suggest that there is limited manoeuvrability space for safe merging.

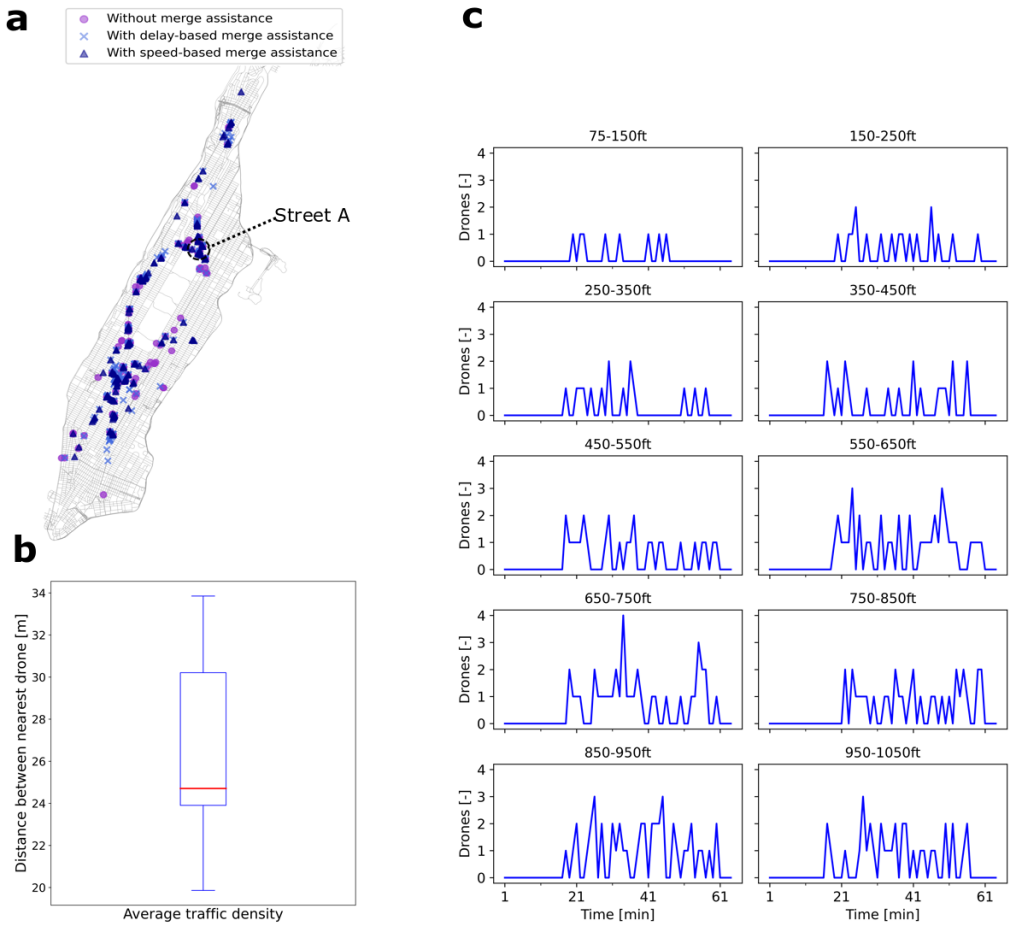

Figure 10. The urban network of Manhattan. (**a**) We overlaid the pairwise intrusions associated without any merge assistance and with delay-based and speed-based merge assist policies. Colours are used to distinguish the different pairwise intrusion categories. The purple marker represent the pairwise intrusions without any merge assistance; the blue cross represents the pairwise intrusions associated with the delay-based merge assist policy; and, the blue triangle marks the pairwise intrusions caused by the use of the speed-based merge assist policy. The darker regions indicate the presence of pairwise intrusions even with the use of delay-based and speed-based merge policies. The map indicates hotspot street at which intrusions are largely prevalent. We identify the street as 'street A', which has a length of 62 m. (**b**) We capture the distance between the nearest drone flying over street A using a box-and-whisker plot. The plot shows that the median is below the horizontal separation margin of 25 m. (**c**) In addition, we capture the traffic accumulation on this particular street. The line plots show that there are instances when there are between two to four drones on the same layer flying over the street.

Furthermore, the simulation results tell us that the topology of the street network should also be taken into account when assessing the performance of the merge assistance policies. In particular, we noticed that the influence of the street network topology, i.e., the length of the streets and the higher number of turns associated with the flight plans, determine whether there is sufficient time for the merge assistance policies to fully respond and thus resolve any merging conflicts.

To investigate this observation, we present a graphical explanation (Figure 11) on why the merge assistance policies might be less effective on short-distance streets. As illustrated in Figure 1, drone 2 merges into the target altitude layer 925 from layer 900. Subsequently, there is also traffic (drone 1) in the target altitude layer, which triggers a merging conflict and intrusion. Due to the relatively shorter distance of the street, the merge assistance policy has insufficient time to resolve the merging conflict before drone 1 leaves the target

altitude layer and turns at the intersection in order respect its flight plan and the topology of the street network. We hypothesise that the inability of the merge assistance policies to completely resolve the conflict and intrusion in short-distance streets could be limiting the effectiveness of the policies.

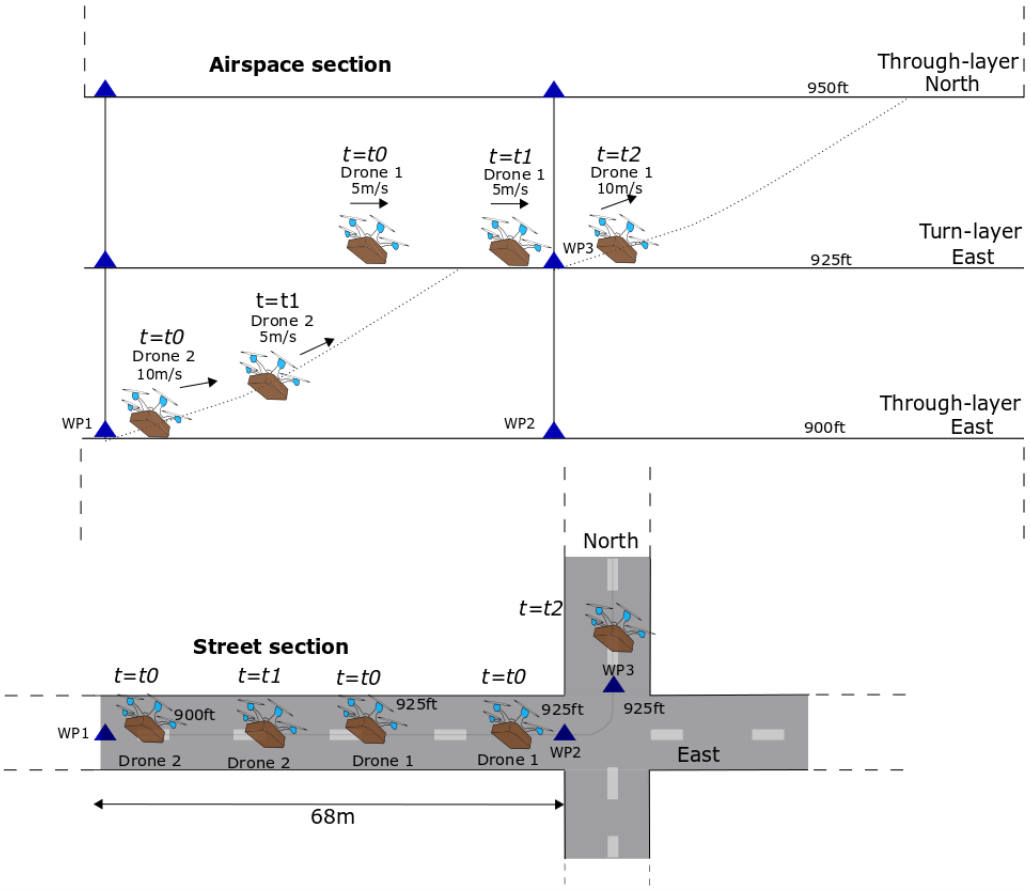

Figure 11. Graphical explanation on a typical short-distance street that shows the merge assistance policies to be less effective because of the inability of the merge assistance policies to fully respond and resolve any merging conflicts.

6. Discussion

Drone-based deliveries are expected to operate in high densities of traffic within constrained urban environments. Last-mile deliveries of small express packages and time-sensitive medical supplies such as vaccines are examples of potential candidates for drone-enabled deliveries. A previous study explored a novel implementation of one-way and two-way streets in combination with altitude-heading rules in an effort to mitigate conflict probabilities [30]. The study was performed on the urban network of Manhattan in order to simulate a constrained airspace. The topography of Manhattan resulted in several turns associated with each flight plan and the use of flight levels, created a large number of merging flight events that required a transition to their respective altitude layers. These merging flights generated the majority of the conflicts and intrusions, especially in close proximity to intersections. However, these merging conflicts were expected since the tactical conflict resolution algorithm had no prior information of potential merging encounters. To improve the safety of the urban airspace design for large-scale drone traffic, this study investigates two merging policies inspired by road traffic studies [32,34,88].

In this research, we applied the one-way airspace design to the urban street network of Manhattan, New York, with an area of 59.1 km^2. We applied a delay-based and a speed-based merge assist strategy in an attempt to reduce the onset of conflicts and intrusions caused by merging flights. Using randomised fast-time simulations, we examined the

performance of the merge assist policies with respect to safety. Here, we compared safety in terms of the total number of pairwise conflicts and intrusions (losses of separation). Our results indicate that the delay-based and speed-based merge assist policies are capable of reducing the total number of pairwise conflicts and intrusions but not to a large extent. The results show that the speed-based merge assist policy has a slightly better performance over the delay-based policy. Furthermore, for both policies, we observed a decrease in the number of in-trail and crossing merging conflicts and intrusions. However, despite this decrease, no dramatic reduction in the total number of intrusions was observed.

The meagre reduction to the total number of conflicts and intrusions was caused by the limited space to safely merge as well as the inability of the merge-assisting policies to fully respond and resolve potential merging conflicts, especially in short-distance streets. Merging events are largely caused by flights that were either climbing or descending to their respective altitude because of the imposed altitude-heading rules and the presence of frequent turns associated with the structure of the airspace. A previous study showed that there are nearly seven turns per flight plan for the one-way concept [30], thereby increasing the probability of conflicts. Similar to road traffic, merge conflicts represent a large percentage of highway collisions [89]. Generally, such merge conflicts are caused by insufficient gaps in the flow of traffic due to high-density of traffic on a particular road segment [32]. In addition, in our study, the merge assist policy only influences the merging vehicle. However, for an effective merge, even the non-merging vehicle should equally be influenced by the merge assist policy, such as, reducing its speed and thus giving way to merging traffic. These types of operational behaviours are commonly found in current road transport where important social cues play a critical role in ensuring a safe merging event [29,54].

To understand the underlying reasons behind the low efficacy in merging intrusions, we investigated one example street in our experimental area by overlaying the locations of intrusions culminating without any merge assistance and with delay-based and speed-based merge assist policies. Even with the use of merge assistance, we identified a number of unresolved intrusions. By examining the urban network through a mesoscopic scale, our results point to two main reasons for the existence of these unresolved intrusions. First, our results show that a particular street (comprising of length between 62 m) can experience high localised traffic flow. Such localised concentration of traffic flow is caused by a particular network property known as high betweenness centrality [84–87]. This means that some links or streets experience a disproportionately higher number of traffic flow as a consequence of greater number of shortest paths passing through a particular street [87]. In general, this could also represent a real-world feature, in which a fleet of drones travel more frequently to a specific destinations due to higher demand. In our study, a drone needs to adhere to a horizontal separation of 25 m (82 ft) in each direction. Therefore, for a relatively shorter street, only one drone can safely be accommodated in its respective altitude layer within the street at any instance in time. Interestingly, our results show that there are instances when there are even two to four drones occupying these particular streets. Furthermore, our results also demonstrate that the distance between the nearest drone on the same altitude layers is far below the horizontal separation margin. Findings of such emergent properties of high localised traffic flow together with smaller distances between drones hence suggest that there is insufficient manoeuvrability space for safe merging, which in turn causes the merge assistance to be less effective in these types of scenarios. In addition, our observations indicate that the large proportion of short-distance streets and the higher number of turns per flight could be a key factors that limits the merge assistance strategies to fully resolve any conflict and intrusions within a given altitude layer. Future research should therefore investigate the performance of the proposed merge assistance policies on an urban network that consists of long-distance streets and with limited number of turns.

In this research we employed a fixed separation margin. However, when compared to road transport, particularly, highway traffic, drivers and advanced adaptive cruise control systems employ a more flexible and dynamic approach to determine a safe horizontal separation margin. For example, on-ground vehicles use the notion of time headway as an

important variable for safe distance keeping [90–92], which is computed by dividing the distance to a lead vehicle by the speed of the following vehicle [92]. The time headway varies with respect to the traffic density, for example, on the highway, in sparse traffic states, larger (>4 s) time headways are observed, while smaller time headways (1–2 s) are experienced in relatively dense traffic states, such as merge lanes and in urban areas [90–92]. In this context, dynamic time headways allow for higher traffic capacity and safety levels [93]. Future research should therefore investigate similar approaches. One starting point for further research is to incorporate and experiment with smaller horizontal separation margins in the turn-layers, where average traffic speeds are relatively low, and hence, we anticipate a marked increase to the efficacy of the merge assist policies. Similarly, the urban street network consists of different street lengths, which might impact the efficiency of the merging policies; future studies should investigate the possibility of developing a merging policy that adapts to the different street lengths. In addition, future studies should investigate methods to proactively manage traffic flow congestion by incorporating strategic flow control [94] or an individual metering strategy to regulate traffic flow [33]. By gaining inspiration from autonomous vehicle research, future work should also study the notion of congestion-aware routing schemes by including the current traffic density of a given route in the cost function in an effort to circumvent the onset of congestion on typical busy streets [95]. Alternatively, further studies should explore a variety of different routing algorithms, such as simplest paths or minimum travel time paths [74,96] as a way to decrease the number of turns, which would reduce the number of merging flights and thus mitigate the probability of conflicts. Another interesting avenue is to extrapolate our methods to dynamic airspace configurations, that is, airspace structures that evolve over time with respect to traffic demand. Current operations of express package delivery of meals and medicine represents a dynamic nature, and thus, they will require a flexible airspace design.

Our results are subject to some limitations. First, our simulations do not include all real-world features that are relevant to the safe accommodation of large-scale drone delivery operation in highly constrained cities. Meteorological events, such as rain and hyperlocal wind, could orchestrate localised traffic congestion by concentrating traffic to specific areas and thus decreasing the overall safety of the airspace. Second, the conflict detection algorithm employed in our experiments linearly extrapolates the drones' states by a prescribed look-ahead time. This obviously has the tendency to trigger false conflicts, which may impact the overall safety of the airspace. Future studies should therefore take into account the drones' intent and flight-path information in order to circumvent false conflict detections. Third, the experiment area used in this study comprises an orthogonal street network. Thus, our findings should be interpreted with due caution when comparing to other types of street networks (see, for instance, [65–67]). To address this limitation, research has already begun to explore these findings to non-orthogonal street networks [72].

7. Conclusions

The possible advent of delivery drones in cities could change the face of urban last-mile delivery. Drone-based delivery could pose as a better alternative, in terms of cost and energy efficiency, than current transport modes, such as vans and bikes. However, society might only benefit from drone deliveries if and when they are able to operate in high densities of traffic, which in turn could lead to several challenges. Here, we aimed to address one main challenge, that is the ability to safely harbour such large-scale drone traffic operations in heavily constrained urban environments. In this context, the current research sheds light on our understanding on the intricate safety properties of operating high traffic densities of autonomous drones in a constrained urban airspace. To this end, we structured and organised the urban airspace of an orthogonal street network with horizontal constraints in an effort to promote one-way traffic flow. In addition to the horizontal constraints, the one-way airspace concept also featured vertically segmented altitude layers to accommodate traffic with similar directions and thus lowering the risks of conflict. By testing the airspace design with three levels of drone delivery traffic densities for the urban street network of

Manhattan, New York, our results showed that most conflicts and losses of separation occur during the merging phase. Fundamentally, this means that introducing altitude-heading rules to structure traffic and thus to mitigate conflicts shifts the occurrence of conflicts to the merging phase. To circumvent the occurrence of merging conflicts and intrusions, we therefore employed a delay-based and speed-based merge-assisting strategy. Our results demonstrated that merge assistance is able to reduce conflicts and intrusion, but to a much lesser extent than anticipated. To explain this relatively low efficacy, we investigated key mesoscopic features, such as hotspot regions that showed high localised traffic flow on particular busy streets of the network; and thus, the data suggest that there is insufficient space to safely merge and the inability for the strategies to fully respond and thus resolve conflicts on short-distance streets. Though the urban airspace concept and merge assist strategies still needs to be investigated for other types of urban networks, and further improvements remain to be made, the findings presented in this study could be useful for advanced air mobility designers and unmanned traffic management policymakers.

Author Contributions: Conceptualisation, M.D., J.E. and J.M.H.; methodology, M.D., J.E. and J.M.H.; software, M.D., J.E. and J.M.H.; validation, M.D., J.E. and J.M.H.; formal analysis, M.D.; investigation, M.D.; data curation, M.D.; writing—original draft preparation, M.D.; writing—review and editing, M.D., J.E. and J.M.H.; visualisation, M.D.; supervision, J.E. and J.M.H. All authors have read and agreed to the published version of the manuscript.

Funding: This research received no external funding.

Institutional Review Board Statement: Not applicable.

Informed Consent Statement: Not applicable.

Data Availability Statement: The data presented in this study can be made available on request from the corresponding author.

Acknowledgments: This work benefited greatly from the open source tools BlueSky, OSMnx, QGIS and their dependencies. We thank the two anonymous reviewers for their helpful comments and feedback on the manuscript. In addition, we thank Marta Ribeiro and Andres Morfin Veytia for helpful observations on various early versions of this paper.

Conflicts of Interest: The authors declare no conflicts of interest.

References

1. Coops, N.; Goodbody, T.R.H.; Lin, C. Four steps to extend drone use in research. *Nature* **2019**, *572*, 433–435. [CrossRef] [PubMed]
2. Frachtenberg, E. Practical drone delivery. *Computer* **2019**, *52*, 53–57. [CrossRef]
3. Fernández-Ruiz, I. Drone delivery of defibrillators for sudden cardiac arrest could shorten response times. *Nat. Rev. Cardiol.* **2021**, *18*, 740. [CrossRef] [PubMed]
4. Schierbeck, S.; Hollenberg, J.; Nord, A.; Svensson, L.; Nordberg, P.; Ringh, M.; Forsberg, S.; Lundgren, P.; Axelsson, C.; Claesson, A. Automated external defibrillators delivered by drones to patients with suspected out-of-hospital cardiac arrest. *Eur. Heart J.* **2021**, *42*, ehab498. [CrossRef] [PubMed]
5. Macrina, G.; Pugliese, L.D.P.; Guerriero, F.; Laporte, G. Drone-aided routing: A literature review. *Transp. Res. Part C Emerg. Technol.* **2020**, *120*, 102762. [CrossRef]
6. Stolaroff, J.K.; Samaras, C.; Mitchell, A.S.; Ceperley, D.; Neill, E.R.O.; Lubers, A. Energy use and life cycle greenhouse gas emissions of drones for commercial package delivery. *Nat. Commun.* **2018**, *9*, 409. [CrossRef]
7. Park, J.; Kim, S.; Suh, K. A comparative analysis of the environmental benefits of drone-based delivery services in urban and rural areas. *Sustainability* **2018**, *10*, 888. [CrossRef]
8. Doole, M.; Ellerbroek, J.; Hoekstra, J. Estimation of traffic density from drone-based delivery in very low level urban airspace. *J. Air Transp. Manag.* **2020**, *88*, 101862. [CrossRef]
9. Petrovsky, A.; Doole, M.; Ellerbroek, J.; Hoekstra, J.M.; Tomasello, F. Challenges with obstacle data for manned and unmanned aviation. *Int. Arch. Photogramm. Remote. Sens. Spat. Inf. Sci. ISPRS Arch.* **2018**, *42*, 143–149. [CrossRef]
10. Watkins, S.; Burry, J.; Mohamed, A.; Marino, M.; Prudden, S.; Fisher, A.; Kloet, N.; Jakobi, T.; Clothier, R. Ten questions concerning the use of drones in urban environments. *Build. Environ.* **2020**, *167*, 106458. [CrossRef]
11. Jang, D.S.; Ippolito, C.A.; Sankararaman, S.; Stepanyan, V. Concepts of Airspace Structures and System Analysis for UAS Traffic flows for Urban Areas. In Proceedings of the AIAA Information Systems-AIAA Infotech@Aerospace, Kissimmee, FL, USA, 8–12 January 2018. [CrossRef]

12. Tony, L.A.; Ratnoo, A.; Ghose, D. Lane Geometry, Compliance Levels, and Adaptive Geo-fencing in CORRIDRONE Architecture for Urban Mobility. In Proceedings of the 2021 International Conference on Unmanned Aircraft Systems (ICUAS), Athens, Greece, 15–18 June 2021; pp. 1611–1617.
13. Hunter, G.; Wei, P. Service-oriented separation assurance for small UAS traffic management. In Proceedings of the 2019 Integrated Communications, Navigation and Surveillance Conference (ICNS), Herndon, VA, USA, 9–11 April 2019; pp. 1–11.
14. Sacharny, D.; Henderson, T, C. A lane-based approach for large-scale strategic conflict management for UAS service suppliers. In Proceedings of the 2019 International Conference on Unmanned Aircraft Systems (ICUAS), Atlanta, GA, USA, 11–14 June 2019.
15. Sacharny, D.; Henderson, T.C.; Cline, M. Large-Scale UAS Traffic Management (UTM) Structure. In Proceedings of the 2020 IEEE International Conference on Multisensor Fusion and Integration for Intelligent Systems (MFI), Karlsruhe, Germany, 14–16 September 2020; pp. 7–12.
16. Low, K.; Gan, L.; Mao, S. *A Preliminary Study in Managing Safe and Efficient Low-Altitude Unmanned Aircraft System Operations in a Densely Built-Up Urban Environment*; Air Traffic Management Research Institute, School of Mechanical and Aerospace Engineering, Nanyang Technological University: Singapore, 2014.
17. Mohamed Salleh, M.F.B.; Wanchao, C.; Wang, Z.; Huang, S.; Tan, D.Y.; Huang, T.; Low, K.H. Preliminary concept of adaptive urban airspace management for unmanned aircraft operations. In Proceedings of the 2018 AIAA Information Systems-AIAA Infotech@Aerospace, Kissimmee, FL, USA, 8–12 January 2018; p. 2260.
18. McCarthy, T.; Pforte, L.; Burke, R. Fundamental elements of an urban UTM. *Aerospace* **2020**, *7*, 85. [CrossRef]
19. Barrado, C.; Boyero, M.; Brucculeri, L.; Ferrara, G.; Hately, A.; Hullah, P.; Martin-Marrero, D.; Pastor, E.; Rushton, A.P.; Volkert, A. U-Space Concept of Operations : A Key Enabler for Opening Airspace to Emerging Low-Altitude Operations. *Aerospace* **2020**, *7*, 24. [CrossRef]
20. Alarcón, V.; García, M.; Alarcón, F.; Viguria, A.; Martínez, Á.; Janisch, D.; Acevedo, J.J.; Maza, I.; Ollero, A. Procedures for the integration of drones into the airspace based on U-space services. *Aerospace* **2020**, *7*, 128. [CrossRef]
21. Capitán, C.; Pérez-León, H.; Capitán, J.; Castaño, Á.; Ollero, A. Unmanned Aerial Traffic Management System Architecture for U-Space In-Flight Services. *Appl. Sci.* **2021**, *11*, 3995. [CrossRef]
22. Sunil, E.; Hoekstra, J.; Ellerbroek, J.; Bussink, F.; Nieuwenhuisen, D.; Vidosavljevic, A.; Kern, S. Metropolis: Relating Airspace Structure and Capacity for Extreme Traffic Densities. In Proceedings of the Europe Air Traffic Management Research and Development Seminar, Lisbon, Portugal, 23–26 June 2015.
23. Sunil, E.; Hoekstra, J.; Ellerbroek, J.; Bussink, F.; Nieuwenhuisen, D.; Vidosavljevic, A.; Kern, S. Analysis of airspace structure and capacity for decentralised separation using fast-time simulations. *J. Guid. Control Dyn.* **2017**, *40*, 38–51. [CrossRef]
24. Hoekstra, J.M.; Maas, J.; Tra, M.; Sunil, E. How do layered airspace design parameters affect airspace capacity and safety? In Proceedings of the 7th International Conference on Research in Air Transportation, Philadelphia, PA, USA, 20–24 June 2016.
25. Hoekstra, J.M.; Ellerbroek, J.; Sunil, E.; Maas, J. Geovectoring: Reducing Traffic Complexity to Increase the Capacity of UAV airspace. In Proceedings of the 2018 International Conference on Research in Air Transportation, Barcelona, Spain, 26–29 June 2018.
26. Garber, N.; Hoel, L. *Traffic & Highway Engineering*; Cengage Learning: Boston, MA, USA, 2008; p. 937.
27. Chakroborty, P.; Das, A. *Principles of Transportation Engineering*; PHI Learning Pvt. Ltd.: New Delhi, India, 2005; p. 520.
28. Urmson, C.; Anhalt, J.; Bagnell, D.; Baker, C.; Bittner, R.; Clark, M.; Dolan, J.; Duggins, D.; Galatali, T.; Geyer, C.; et al. Autonomous driving in urban environments: Boss and the urban challenge. *J. Field Robot.* **2008**, *25*, 425–466. [CrossRef]
29. Hancock, P.A.; Nourbakhsh, I.; Stewart, J. On the future of transportation in an era of automated and autonomous vehicles. *Proc. Natl. Acad. Sci. USA* **2019**, *116*, 7684–7691. [CrossRef]
30. Doole, M.; Ellerbroek, J.; Knoop, V.L.; Hoekstra, J.M. Constrained Urban Airspace Design for Large-Scale Drone-Based Delivery Traffic. *Aerospace* **2021**, *8*, 38. [CrossRef]
31. Doole, M.; Ellerbroek, J.; Hoekstra, J. Drone delivery: Nature of traffic conflicts in constrained urban airspace environments. In Proceedings of the Delft International Conference on Urban Air Mobility (DICUAM), Delft, The Netherlands, 15–17 March 2021.
32. Knoop, V.L. *Introduction to Traffic Flow Theory*; Course Textbook; Delft University of Technology: Delft, The Netherlands, 2017; pp. 13–14.
33. Knoop, V.L.; Duret, A.; Buisson, C.; van Arem, B. Lane distribution of traffic near merging zones influence of variable speed limits. In Proceedings of the 13th International IEEE Conference on Intelligent Transportation Systems, Madeira Island, Portugal, 19–22 September 2010; pp. 485–490. [CrossRef]
34. Rios-Torres, J.; Malikopoulos, A.A. A survey on the coordination of connected and automated vehicles at intersections and merging at highway on-ramps. *IEEE Trans. Intell. Transp. Syst.* **2016**, *18*, 1066–1077. [CrossRef]
35. Goli, M.; Eskandarian, A. Merging strategies, trajectory planning and controls for platoon of connected, and autonomous vehicles. *Int. J. Intell. Transp. Syst. Res.* **2020**, *18*, 153–173. [CrossRef]
36. Doole, M.; Ellerbroek, J.; Hoekstra, J. Drone delivery: Urban airspace traffic density estimation. In Proceedings of the SESAR Innovation Days, Salzburg, Austria, 3–6 December 2018.
37. Straubinger, A.; Rothfeld, R.; Shamiyeh, M.; Büchter, K.D.; Kaiser, J.; Plötner, K.O. An overview of current research and developments in urban air mobility–Setting the scene for UAM introduction. *J. Air Transp. Manag.* **2020**, *87*, 101852. [CrossRef]

38. Thipphavong, D.P.; Apaza, R.; Barmore, B.; Battiste, V.; Burian, B.; Dao, Q.; Feary, M.; Go, S.; Goodrich, K.H.; Homola, J.; et al. Urban air mobility airspace integration concepts and considerations. In Proceedings of the 2018 Aviation Technology, Integration, and Operations Conference, Atlanta, GA, USA, 25–29 June 2018; p. 3676.
39. Sunil, E. Analyzing and Modeling Capacity for Decentralized Air Traffic Control. Ph.D Thesis, TU Delft, Delft, The Netherlands, 2019. [CrossRef]
40. Slinn, M.; Matthews, P.; Guest, P. *Traffic Engineering Design: Principles and Practice*; Butterworth-Heinemann: Oxford, UK, 2005; pp. 76–163. [CrossRef]
41. Kutz, M. *Handbook of Transportation Engineering*; McGraw-Hill: New York, NY, USA, 2013; Volume 42, p. 363. [CrossRef]
42. Gayah, V.V.; Daganzo, C.F. Analytical Capacity Comparison of One-Way and Two-Way Signalized Street Networks. *Transp. Res. Rec. J. Transp. Res. Board* **2012**, *2301*, 76–85. [CrossRef]
43. Ortigosa, J.; Gayah, V.V.; Menendez, M. Transportmetrica B : Transport Dynamics Analysis of one-way and two-way street configurations on urban grid networks ABSTRACT. *Transp. B Transp. Dyn.* **2019**, *7*, 61–81. [CrossRef]
44. Stemley, J.J. One-way streets provide superior safety and convenience. *ITE J.* **1998**, *68*, 47–50.
45. Boeing, G. Urban spatial order: Street network orientation, configuration, and entropy. *Appl. Netw. Sci.* **2019**, *4*, 67. [CrossRef]
46. Xu, C.; Member, S.; Liao, X. Recent Research Progress of Unmanned Aerial Vehicle Regulation Policies and Technologies in Urban Low Altitude. *IEEE Access* **2020**, *8*, 74175–74194. [CrossRef]
47. Vásárhelyi, G.; Virágh, C.; Somorjai, G.; Nepusz, T.; Eiben, A.E.; Vicsek, T. Optimized flocking of autonomous drones in confined environments. *Sci. Robot.* **2018**, *3*, eaat3536. [CrossRef] [PubMed]
48. Hoekstra, J.M.; Ellerbroek, J. Aerial Robotics: State-based Conflict Detection and Resolution (Detect and Avoid) in High Traffic Densities and Complexities. *Curr. Robot. Rep.* **2021**, *2*, 297–307. [CrossRef]
49. Tielrooij, M.; Veld, A.C.I.T.; Van Paassen, M.M.; Mulder, M. Development of a Time-Space Diagram to Assist Air Traffic Controllers in Monitoring Continuous Descent Approaches. In *Air Traffic Control*; IntechOpen: London, UK, 2010.
50. Klomp, R.; Riegman, R.; Borst, C.; Mulder, M.; Van Paassen, M. Solution space concept: Human-machine interface for 4D trajectory management. In Proceedings of the Thirteenth USA/Europe Air Traffic Management Research and Development Seminar (ATM2019), Vienna, Austria, 17–21 June 2019; No. 58, pp. 17–21.
51. Anwar, A.; Zeng, W.; Arisona, S.M. Time–Space Diagram Revisited. *Transp. Res. Rec.* **2014**, *2442*, 1–7. [CrossRef]
52. De Leege, A.; Paassen, M.v.; Veld, A.i.; Mulder, M. Time–Space Diagram as Controller Support Tool for Closed-Path Continuous-Descent Operations. *J. Aircr.* **2013**, *50*, 1394–1408. [CrossRef]
53. Drew, D.R.; LaMotte, L.R.; Buhr, J.; Wattleworth, J. Gap acceptance in the freeway merging process. *Highw. Res. Rec.* **1967**, *208*, 1–36.
54. Schwarting, W.; Pierson, A.; Alonso-Mora, J.; Karaman, S.; Rus, D. Social behavior for autonomous vehicles. *Proc. Natl. Acad. Sci. USA* **2019**, *116*, 24972–24978. [CrossRef] [PubMed]
55. Hoekstra, J.; Ellerbroek, J. BlueSky ATC Simulator Project: An Open Data and Open Source Approach. In Proceedings of the Seventh International Conference for Research on Air Transport (ICRAT), Philadelphia, PA, USA, 20–24 June 2016.
56. BlueSky. TUDelft-CNS-ATM/BlueSky. 2020. Available online: https://github.com/TUDelft-CNS-ATM/bluesky (accessed on 10 November 2021).
57. Krader, K. Uber wants your next big mac to be delivered by drone. *Bloomberg Businessweek*, 12 June 2019.
58. Hampson, M. Drone delivers human kidney: The organ was flown several kilometers by a drone without incurring damage-[News]. *IEEE Spectr.* **2018**, *56*, 7–9. [CrossRef]
59. Ding, Y. E-Commerce Giant JD.com's New Delivery Drone Takes Flight. 2021. Available online: https://www.caixinglobal.com/2020-12-25/e-commerce-giant-jdcoms-new-delivery-drone-takes-flight-101643197.html (accessed on 19 January 2021).
60. Gudmundsson, A.; Mohajeri, N. Entropy and order in urban street networks. *Sci. Rep.* **2013**, *3*, 3324. [CrossRef] [PubMed]
61. Boeing, G. Exploring Urban Form through OpenStreetMap Data : A Visual Introduction. In *Urban Experience and Design: Comtemporary Perspectives on Improving the Public Realm*; Routledge: New York, NY, USA, 2020; pp. 167–184.
62. Rajendran, S.; Zack, J. Insights on strategic air taxi network infrastructure locations using an iterative constrained clustering approach. *Transp. Res. Part E Logist. Transp. Rev.* **2019**, *128*, 470–505. [CrossRef]
63. Rajendran, S.; Shulman, J. Study of emerging air taxi network operation using discrete-event systems simulation approach. *J. Air Transp. Manag.* **2020**, *87*, 101857. [CrossRef]
64. Alvarez, L.E.; Jones, J.C.; Bryan, A.; Weinert, A.J. Demand and Capacity Modeling for Advanced Air Mobility. In Proceedings of the AIAA AVIATION 2021 FORUM, Online, 2–6 August 2021; p. 2381.
65. Barrington-leigh, C.; Millard-ball, A. A century of sprawl in the United States. *Proc. Natl. Acad. Sci. USA* **2015**, *112*, 8244–8249. [CrossRef]
66. Barrington-Leigh, C.; Millard-Ball, A. More connected urban roads reduce US GHG emissions. *Environ. Res. Lett.* **2017**, *12*, 044008. [CrossRef]
67. Barrington-Leigh, C.; Millard-Ball, A. Global trends toward urban street-network sprawl. *Proc. Natl. Acad. Sci. USA* **2020**, *117*, 1941–1950. [CrossRef]
68. Haklay, M.; Weber, P. Openstreetmap: User-generated street maps. *IEEE Pervasive Comput.* **2008**, *7*, 12–18. [CrossRef]
69. Boeing, G. Computers , Environment and Urban Systems OSMnx: New methods for acquiring, constructing, analyzing , and visualizing complex street networks. *Comput. Environ. Urban Syst.* **2017**, *65*, 126–139. [CrossRef]

70. Hoekstra, J.M.; Van Gent, R.N.; Ruigrok, R.C. Designing for safety: The 'free flight' air traffic management concept. *Reliab. Eng. Syst. Saf.* **2002**, *75*, 215–232. [CrossRef]
71. Ribeiro, M.; Ellerbroek, J.; Hoekstra, J. Review of conflict resolution methods for manned and unmanned aviation. *Aerospace* **2020**, *7*, 79. [CrossRef]
72. Badea, C.A.; Veytia, A.M.; Ribeiro, M.; Doole, M.; Ellerbroek, J.; Hoekstra, J. Limitations of Conflict Prevention and Resolution in Constrained Very Low-Level Urban Airspace. In Proceedings of the 11th SESAR Innovation Days, Online, 7–9 December 2021.
73. Bulusu, V. Urban air mobility: Deconstructing the next revolution in urban transportation—feasibility, capacity and productivity. Ph.D. Thesis, University of California, Berkeley, CA, USA, 2019.
74. Hagberg, A.; Schult, D.; Swart, P. Exploring network structure, dynamics, and function using NetworkX. In Proceedings of the 7th Python in Science Conference (SciPy2008), Pasadena, CA, USA, 19–24 August 2008; Volume 836, pp. 11–15.
75. Matter, D.; Potgieter, L. Allocating epidemic response teams and vaccine deliveries by drone in generic network structures, according to expected prevented exposures. *PLoS ONE* **2021**, *16*, e0248053. [CrossRef] [PubMed]
76. Krozel, J.; Peters, M.; Bilimoria, K.D.; Field, M.; Lee, C.; Mitchell, J.S.B. System Performance Characteristics of Centralized and Decentralized Air Traffic Separation Strategies. In Proceedings of the 4th USA/Europe Air Traffic Management R&D Seminar, Santa Fe, NM, USA, 3–7 December 2001; pp. 1–11.
77. Jardin, M.R. Analytical Relationships Between Conflict Counts and Air-Traffic Density. *J. Guid. Control. Dyn.* **2005**, *28*, 1150–1156. [CrossRef]
78. Shortle, J.; Belle, A. A methodology for estimating the probability of potential secondary conflicts. In Proceedings of the 2013 IEEE/AIAA 32nd Digital Avionics Systems Conference (DASC), East Syracuse, NY, USA, 5–10 October 2013; p. 6C2-1.
79. Parker, M., Jr.; Zegeer, C.V. *Traffic Conflict Techniques for Safety and Operations: Observers Manual*; Technical Report; Federal Highway Administration: Washington, DC, USA, 1989.
80. Katamine, N. Nature and frequency of secondary conflicts at unsignalized intersections. *J. Transp. Eng.* **2000**, *126*, 129–133. [CrossRef]
81. Flenniken, J.M.; Stuglik, S.; Iannone, B.V. Quantum GIS (QGIS): An introduction to a free alternative to more costly GIS platforms: FOR359/FR428, 2/2020. *EDIS* **2020**, *2020*, 7. [CrossRef]
82. Xie, Z.; Yan, J. Kernel density estimation of traffic accidents in a network space. *Comput. Environ. Urban Syst.* **2008**, *32*, 396–406. [CrossRef]
83. Chen, W.; Guo, F.; Wang, F.Y. A survey of traffic data visualization. *IEEE Trans. Intell. Transp. Syst.* **2015**, *16*, 2970–2984. [CrossRef]
84. Barthélemy, M. Spatial networks. *Phys. Rep.* **2011**, *499*, 1–101. [CrossRef]
85. Batty, M. *The New Science of Cities*; MIT Press: Cambridge, MA, USA, 2013.
86. Barthelemy, M. *The Structure and Dynamics of Cities*; Cambridge University Press: Cambridge, UK, 2016.
87. Kirkley, A.; Barbosa, H.; Barthelemy, M.; Ghoshal, G. From the betweenness centrality in street networks to structural invariants in random planar graphs. *Nat. Commun* **2018**, *9*, 2501. [CrossRef] [PubMed]
88. Wang, Z.; Kulik, L.; Ramamohanarao, K. Proactive traffic merging strategies for sensor-enabled cars. In *Automotive Informatics and Communicative Systems: Principles in Vehicular Networks and Data Exchange*; IGI Global: Hershey, PA, USA, 2009; pp. 180–199.
89. Yang, H.; Ozbay, K. Estimation of Traffic Conflict Risk for Merging Vehicles on Highway Merge Section. *Transp. Res. Rec.* **2011**, *2236*, 58–65. [CrossRef]
90. Neubert, L.; Santen, L.; Schadschneider, A.; Schreckenberg, M. Single-vehicle data of highway traffic: A statistical analysis. *Phys. Rev. E* **1999**, *60*, 6480. [CrossRef] [PubMed]
91. Ayres, T.; Li, L.; Schleuning, D.; Young, D. Preferred time-headway of highway drivers. In Proceedings of the ITSC 2001, 2001 IEEE Intelligent Transportation Systems (Cat. No. 01TH8585), Oakland, CA, USA, 25–29 August 2001; pp. 826–829.
92. Siebert, F.W.; Oehl, M.; Pfister, H.R. The influence of time headway on subjective driver states in adaptive cruise control. *Transp. Res. Part F Traffic Psychol. Behav.* **2014**, *25*, 65–73. [CrossRef]
93. Milakis, D.; Van Arem, B.; Van Wee, B. Policy and society related implications of automated driving: A review of literature and directions for future research. *J. Intell. Transp. Syst.* **2017**, *21*, 324–348. [CrossRef]
94. Chin, C.; Gopalakrishnan, K.; Balakrishnan, H.; Egorov, M.; Evans, A. Efficient and fair traffic flow management for on-demand air mobility. *CEAS Aeronaut. J.* **2021**, 1–11. [CrossRef]
95. Salazar, M.; Tsao, M.; Aguiar, I.; Schiffer, M.; Pavone, M. A congestion-aware routing scheme for autonomous mobility-on-demand systems. In Proceedings of the 2019 18th European Control Conference (ECC), Naples, Italy, 25–28 June 2019; pp. 3040–3046.
96. Viana, M.P.; Strano, E.; Bordin, P.; Barthelemy, M. The simplicity of planar networks. *Sci. Rep.* **2013**, *3*, 3495. [CrossRef]